Int. J. Heat Mass Transfer. Vol. 36, No. 8, pp. 2175–2182, 1993
Printed in Great Britain

0017-9310/93 $6.00+0.00

Transient cooling of petroleum by natural convection in cylindrical storage tanks—II. Effect of heat transfer coefficient, aspect ratio and temperature-dependent viscosity

MARK A. COTTER
Automotive Parts Manufacturers' Association, 195 The West Mall, Suite 516, Toronto, Ontario, M9C 5K1, Canada

and

MICHAEL E. CHARLES
Department of Chemical Engineering and Applied Chemistry, University of Toronto, Toronto, Ontario, M5S 1A4, Canada

(*Received* 24 *April* 1992 *and in final form* 17 *July* 1992)

Abstract—The transient natural convection of a warm crude oil contained in a large vertical cylindrical storage tank located in a cold environment is investigated numerically. The effect of the external heat transfer coefficient is examined by using four different values. Increasing this parameter is found to increase the rate of heat loss as expected, but only a minor effect on the resulting fluid flow is found. The effect of the tank aspect ratio (height to radius) on the natural convection process is investigated by using four different aspect ratios ranging from 0.25 to 2.0, and is found to affect the flow patterns that develop. Two recirculating cells arise for the aspect ratios of 0.25, 0.5 and 1.0, while a single cell arises in the case of aspect ratio of 2.0. The effect of the fluid viscosity is examined for a tank of aspect ratio 0.5 by using five different apparent viscosity–temperature relationships. The increase in fluid viscosity concomitant with cooling is found to significantly slow down the rate of heat loss from the tank compared to the constant viscosity case.

INTRODUCTION

THE TRANSIENT cooling of petroleum in a storage tank is a concern in geographical regions where ambient temperatures are often well below the pour point temperature of the stored petroleum. This is the case in the Canadian Arctic, where a recently-produced crude oil is relatively warm compared to the external environment. If short-term storage of the crude oil is required before it can be transported to market, the temperature difference between the warm crude oil and the cold environment can initiate the natural convection of the crude oil inside the tank.

In an earlier paper [1], a numerical simulator for this transient natural convection process was developed which employs a temperature-dependent apparent viscosity to model the change in fluid rheology that occurs with cooling. Small scale experimental results were compared with simulator predictions and good agreement was achieved, thereby lending confidence to the validity of the model. Subsequently, the numerical simulator was used to make predictions regarding the transient cooling of crude oil in a field-scale storage situation, specifically a 42 400 m^3 tank.

In this work, the effect of the external heat transfer coefficient on the solution is examined using four different sidewall coefficients. The effect of the tank aspect ratio (height to radius) is also investigated. The focus is maintained on the range of aspect ratios suitable for petroleum storage tanks. Four different ratios ranging from 0.25 to 2.0 are used, with dimensions picked so that all contain the same volume of crude oil. In addition, the effect of the temperature-dependent viscosity relationship is examined using five different relationships. Two of these relationships are constant viscosity cases, to analyze the effect of changing viscosity.

The formulation of the problem analyzed here is described in greater detail elsewhere [1].

RESULTS AND DISCUSSION

Effect of heat transfer coefficient

In the natural convection simulator, the thermal boundary conditions at the top surface, sidewall and base of the tank are that the heat loss at that surface is proportional to the local temperature gradient. This proportionality is represented by an overall heat transfer coefficient which encompasses the resistance of the wall and the external resistance. The effect of the magnitude of this heat transfer coefficient on the simulation results is investigated here.

NOMENCLATURE

- Bi Biot number
- h heat transfer coefficient [W m^{-2} K^{-1}]
- H wet height of cylinder [m]
- k thermal conductivity of fluid [W m^{-1} K^{-1}]
- Nu Nusselt number
- q heat flux [W m^{-2}]
- T temperature [K]
- r dimensionless radial coordinate
- z dimensionless axial coordinate.

Greek symbols

- η apparent viscosity [Pa s]
- θ dimensionless temperature
- $\bar{\theta}$ average dimensionless temperature.

Subscripts

- b bulk fluid
- c cold ambient
- i interior of the tank sidewall
- w wall of the tank
- 0 initial.

The number of possible permutations and combinations of heat transfer coefficients for the three surfaces are infinite; the interest here is focussed by the practical application to the problem of the storage of petroleum in a cylindrical tank. The heat transfer coefficient for the bottom of the tank is kept fixed at 0.3 W m^{-2} K^{-1}, which is consistent with a tank situated on a 1.5 m base of gravel overlying permafrost. The rate of heat transfer at the top surface is controlled by the size of the vapour space above the liquid surface, the resistance due to the tank roof and the external conditions. It is assumed here that the vapour space is of constant size and that it is impractical to provide insulation for the tank roof. Since the effect of the external conditions on the heat loss in this direction is moderated by the vapour space, the heat transfer coefficient at the top surface is also kept fixed. A value of 3.0 W m^{-2} K^{-1} is used.

Therefore, the effect of the heat transfer coefficient at the sidewall becomes the focus of this study. Four different values of this heat transfer coefficient are used, in separate simulations. The first case has already been studied, where h_w is taken to be 11.0 W m^{-2} K^{-1}. A higher value of 15 W m^{-2} K^{-1} is chosen to examine the effect of underestimating a parameter such as the speed of the wind blowing on the tank. Two lower values of 8.0 W m^{-2} K^{-1} and 3.0 W m^{-2} K^{-1} are used to study the effect of insulation for the sidewalls, corresponding to approximately 75 mm and 150 mm of fibreglass insulation, respectively, around the tank perimeter.

Figure 1(a) displays how the mean tank temperature varies with time for the four different simulations. It is apparent that over a long period of time, the effect of the external heat transfer coefficient is insignificant—all the simulations predict about 240 days to lose 95% of the heat. The major effect of the heat transfer coefficient appears to be on the early rate of cooling. It is apparent that the time required to cool halfway to the ambient temperature varies from about ten days for an h_w of 15 W m^{-2} K^{-1} to about thirty days for an h_w of 3.0 W m^{-2} K^{-1}. This could be an important consideration for storage situations where the crude oil exhibits some irreversible wax deposition at a characteristic temperature that lies between the initial and ambient temperatures. The desirability to extend the storage time before such a change occurs might justify the cost of exterior wall insulation in some cases.

The effect of the external heat transfer coefficient on the rate of heat transfer at the interior of the sidewall is examined by defining an internal wall heat transfer coefficient, h_i, according to,

$$h_i = \frac{q_w}{(T_b - T_w)} = \frac{h_w(T_w - T_c)}{(T_b - T_w)} \qquad (1)$$

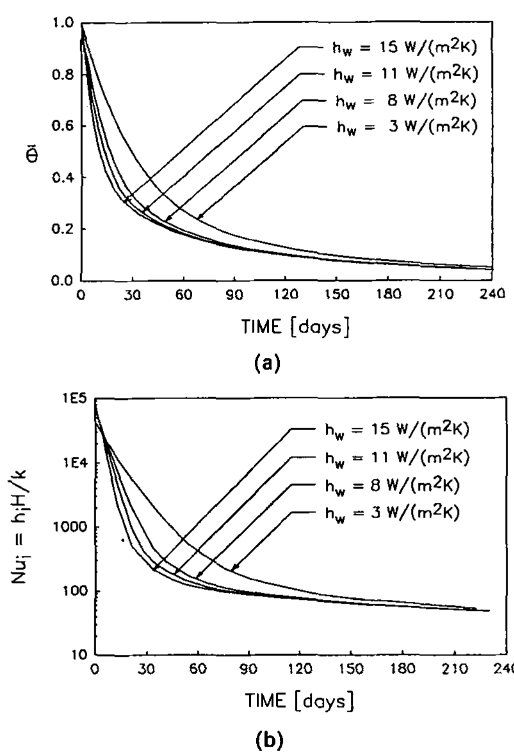

FIG. 1. The effect of the external heat transfer coefficient on cooling: (a) mean tank temperature vs time; and (b) internal sidewall Nusselt number vs time.

where T_b is the mean temperature of the liquid bulk (that is, not in the boundary layer), T_w is the wall temperature, and T_c is the cold ambient temperature. A Nusselt number for the sidewall interior is calculated as,

$$Nu = \frac{h_i H}{k} = \frac{h_w (T_w - T_c) \cdot H}{k(T_b - T_w)} = Bi_w \cdot \frac{(T_w - T_c)}{(T_b - T_w)}. \tag{2}$$

Equation (2) defines a local Nusselt number, since both the wall temperature and the wall temperature gradient vary with tank height. A mean wall internal Nusselt number is defined by integrating over the sidewall. This can be written in terms of dimensionless variables:

$$Nu_i = \int_0^1 \frac{Bi_w \cdot \theta_w}{(\theta_b - \theta_w)} \cdot dz = \frac{Bi_w \cdot \bar{\theta}_w}{(\theta_b - \bar{\theta}_w)} \tag{3}$$

where $\bar{\theta}_w$ denotes the mean sidewall temperature and θ_b denotes the bulk fluid temperature.

Figure 1(b) displays how the Nusselt number at the wall varies with time for the four different external heat transfer coefficients. Over the long term, the external heat transfer coefficient has little effect on the internal Nusselt number. However, for times less than 90 days, it is apparent that an increase in the external wall heat transfer coefficient results in a decrease in the sidewall internal Nusselt number. This is easily explained by looking at the response of the wall temperature to an increase in the external heat transfer coefficient.

As h_w is increased, θ_w decreases since heat is removed more efficiently. From equation (3), it is apparent that the increase in Bi_w concomitant with the increase in h_w is more than compensated by the decrease in $\bar{\theta}_w$ and the increase in $(\theta_b - \bar{\theta}_w)$, so that an overall decrease in the internal Nusselt number results.

The colder wall temperature due to the higher external wall heat transfer coefficient provides a greater driving force for convection. An increase in convection is noted in the analysis of the streamlines.

Since the fluid properties and tank dimensions are constant for each simulation, quantitative comparisons of the dimensionless stream function contours may be made. However, because each simulation cools at a different rate, a comparison at a specific time will correspond to different mean tank temperatures and thus different stages of flow evolution.

The general flow structure remains qualitatively the same for each simulation. The maximum value of the stream function over the entire simulation is found in each case to be about 3.7×10^{-3}. In each case this maximum occurs before 1 h, but it is reached slightly sooner for the higher heat transfer coefficient runs. Figure 2 shows a plot of streamlines after 1 h for the intermediate sidewall heat transfer coefficient value of 8.0 W m^{-2} K^{-1}. Two countercurrent rotating cells are apparent, with the zero level contour delineating the boundary between them. The dominant cell near the sidewall flows in a clockwise rotation, driven by the heat loss at the sidewall. The second cell in the centreline region flows in a counterclockwise manner. The other simulations utilizing different sidewall heat transfer coefficients exhibit a similar pattern with approximately the same flow velocities near the sidewall. Also, the structure and location of the second convective cell near the centreline appear not to depend on the heat transfer coefficient at the wall for the range of values studied.

The flow development in each simulation proceeds temporally in an analogous manner. As the tank cools the vortices shift upward toward the top surface. Figure 3 shows streamlines after approximately 20 days for wall heat transfer coefficients of 15 and 3 W m^{-2} K^{-1}, respectively. Again, the qualitative shape of the streamlines remains the same, but the magnitude of the contours is different because the mean tank temperatures are not equal at this time. The higher heat

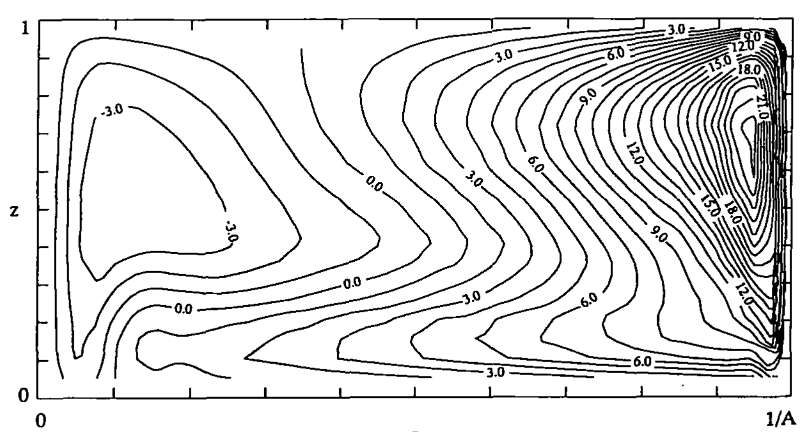

FIG. 2. Streamlines × 10^4 for h_w of 8.0 W m^{-2} K^{-1} after 1 h. The mean tank temperature is 0.998.

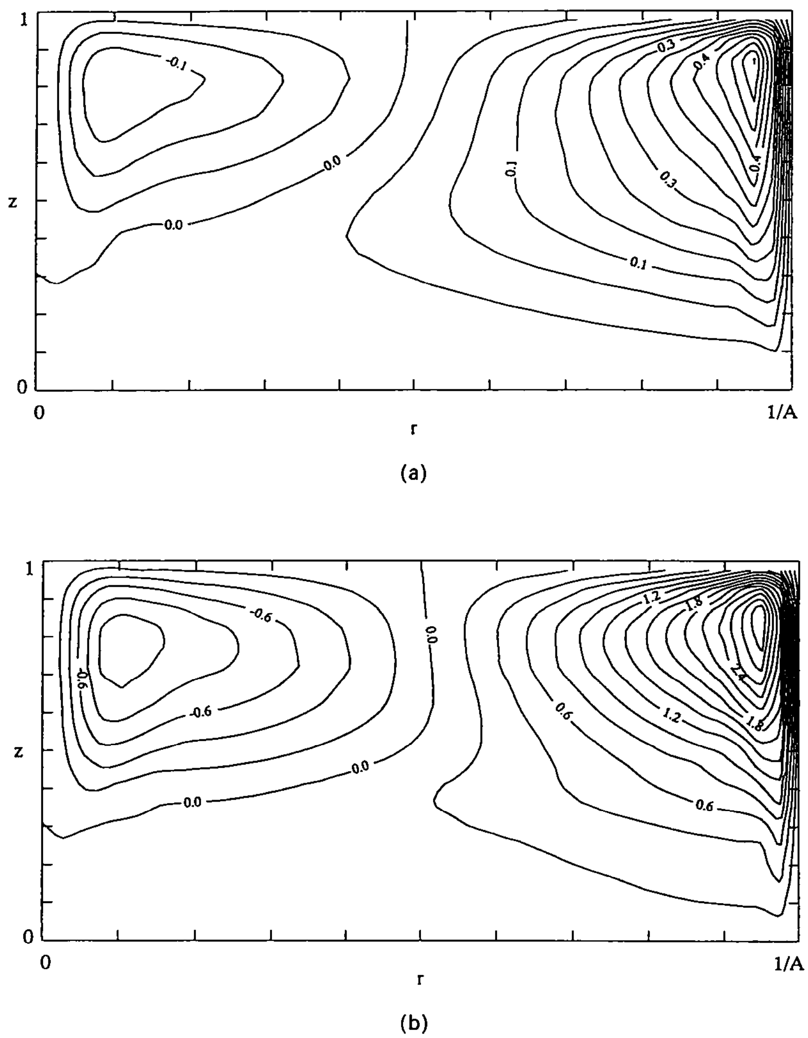

FIG. 3. A comparison of streamlines × 10^4 after 20 days for: (a) h_w of 15 W m^{-2} K^{-1}, at which time the mean tank temperature was 0.334; and (b) h_w of 3.0 W m^{-2} K^{-1}, at which time the mean tank temperature was 0.602.

transfer coefficient case has cooled to a greater extent and thus the driving force for convection at that time is considerably diminished.

In summary, it appears that a fivefold increase in the magnitude of the wall heat transfer coefficient has little effect on the flow structure, influencing primarily the rate of cooling of the tank contents, as expected. However, from the mean tank temperature plots it is apparent that over a long period of time even this effect is diminished. The tank contents cool to the ambient temperature asymptotically, and the effect of the wall heat transfer coefficient on the rate of heat loss is most pronounced in the early stages of cooling. This may be of some significance when considering the cost/benefit of attempting to reduce the heat loss at the wall. It appears that insulation would be most effective in the early stages of cooling. Hence, it might be useful in extending the length of time that the crude oil stays above some critical temperature that is close to the initial temperature.

Effect of aspect ratio

The effect of four different tank aspect ratios on the results of a natural convection simulation is examined. The volume of the tank is kept constant for the four different aspect ratios so that the cooling rates can be compared. Thus for aspect ratios of one-quarter, one-half, one and two, the wet heights are 9.50 m, 15.0 m, 23.8 m and 37.8 m, respectively. The number of grid points in each direction is adjusted for each aspect ratio in order to keep the average grid spacing approximately constant.

The external heat transfer coefficients for the top surface, sidewall and tank bottom are taken to be 3.0,

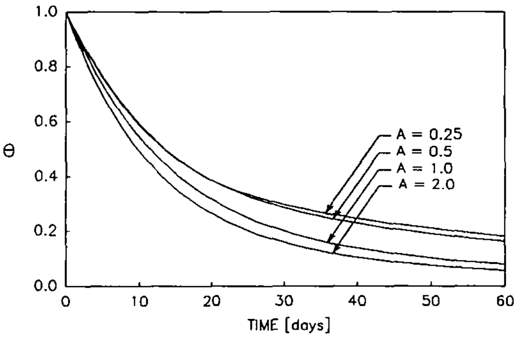

FIG. 4. A comparison of mean tank temperatures vs time for tank aspect ratio as a parameter.

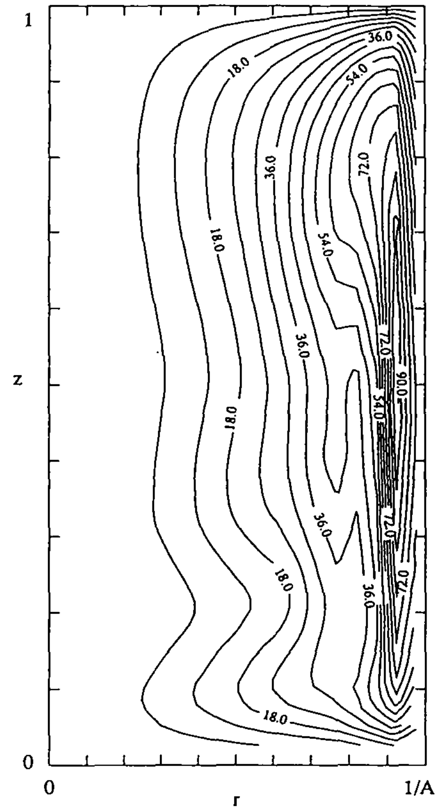

FIG. 5. Streamlines $\times 10^6$ for the tank aspect ratio of 2.0 after 1 h. The Grashof number for this simulation is 1.32×10^9.

11.0 and 0.3 W m^{-2} K^{-1} respectively. These were obtained from correlations assuming an uninsulated tank situated on a gravel bed. Fluid properties were taken to be those of the Benthorn crude oil as outlined elsewhere [2].

For the above heat transfer coefficients, it is clear that the overall rate of heat loss can be retarded by minimizing the sidewall area since the rate of heat loss is greatest in that direction. This is indeed what occurs. Figure 4 shows a comparison of the rates of cooling for the four aspect ratios. The tank of aspect ratio of 2.0 cools at the fastest rate since the sidewall area is the largest of the four cases. The smaller aspect ratio tanks in turn cool less quickly, with the tank of aspect ratio 0.25 cooling at the lowest rate.

The convective flow pattern that arises from this storage situation changes fundamentally over the range of aspect ratios studied. When comparing the flow patterns, it should be noted that since the tank dimensions are different (volume is kept constant), the Grashof number for each simulation is different. However, the results indicate that the maximum velocities do not vary significantly for the aspect ratios studied. In all four cases, the maximum radial velocity is about 0.05 m s^{-1} while the maximum vertical velocity is approximately 0.1 m s^{-1}.

Qualitatively, however, the flow patterns differ. For the 'short' aspect ratios of 0.25 and 0.50, the flow is characterized by two distinct recirculating cells, as displayed earlier in the analysis of the effect of the heat transfer coefficient. With the aspect ratio of unity, the counterclockwise-rotating cell in the centreline region still exists, but it is of diminished size relative to wall-driven cell, when compared to the results from the smaller aspect ratio tanks.

Figure 5 shows a plot of streamlines after 1 h for the tank of aspect ratio 2.0. A secondary cell in the top centreline region is noticeably absent. With this 'tall' aspect ratio, it seems that the downward pull of the flow at the sidewall is sufficiently close to the centreline that the formation of a secondary cell is precluded. This is what one would expect in the limiting case, but here it is apparent that the transition occurs somewhere between an aspect ratio of one and two for the conditions studied.

In summary, for the tank aspect ratio range of one-quarter to two, the smaller aspect ratio tanks cool more slowly. This is expected since the rate of heat loss at the sidewall is the largest and the smaller aspect ratios have smaller sidewall areas. The effect of this parameter on the maximum velocities in the tank is not significant, but there is an effect on the circulation pattern. For an aspect ratio of 2.0, a secondary cell near the centreline does not develop as it does for the 'shorter' aspect ratios of 0.25, 0.50, and 1.0.

Effect of temperature-dependent viscosity

The effect of five different apparent viscosity–temperature relationships on the natural convection simulator is examined. Figure 6 shows the Benthorn apparent viscosity–temperature data measured using a Haake cone-and-plate viscometer over a range of shear rates as described elsewhere [2]. The symbols correspond to actual shear stress vs shear rate measurements while the solid lines correspond to five possible viscosity–temperature relationships:

$$\eta_1 = 5.57 \times 10^{-17} \exp\left(\frac{13\,360}{T}\right) \quad [\text{mPa s}] \qquad (4)$$

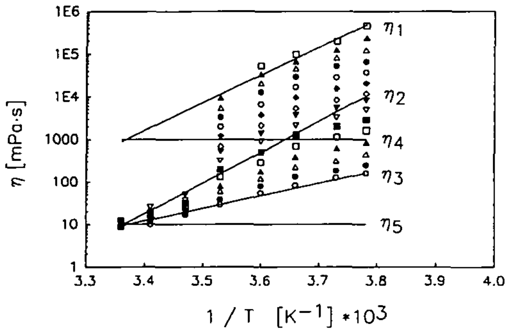

FIG. 6. Apparent viscosity vs the inverse of temperature for Benthorn crude oil. Data collected with the Haake viscometer and five possible apparent viscosity–temperature relationships.

$$\eta_2 = 9.80 \times 10^{-24} \exp\left(\frac{16\,450}{T}\right) \quad [\text{mPa s}] \tag{5}$$

$$\eta_3 = 1.48 \times 10^{-9} \exp\left(\frac{6720}{T}\right) \quad [\text{mPa s}] \tag{6}$$

$$\eta_4 = 1.00 \times 10^{3} \quad [\text{mPa s}] \tag{7}$$

$$\eta_5 = 10.0 \quad [\text{mPa s}]. \tag{8}$$

Equation (4) is the rheological equation which conforms to the low shear rate data that was used for the previous Benthorn simulations examining the effect of the tank aspect ratio. Equation (5) results from fitting a line through the middle of the data, while equation (6) is obtained from the high shear rate data. Equations (7) and (8) describe constant viscosity relationships for comparison.

Initially, simulations of the cooling of crude oil in a 60 m diameter tank filled to a level of 15 m were performed. However, the very large Grashof numbers that arise when utilizing equations (5), (7) and (8) for the apparent viscosity (due to the low initial viscosity), resulted in numerical difficulties that are explained in more detail elsewhere [2]. For this reason, simulations were undertaken of the cooling of a tank of 2.0 m diameter filled to a level of 0.5 m, for which the simulation Grashof numbers are less extreme.

The heat transfer coefficients at the top surface, sidewall and bottom were 3.0, 11.0 and 0.3 W m^{-2} K^{-1}, respectively. Fluid properties, other than the viscosity, were taken to be those of the Benthorn crude as outlined earlier. For the viscosity, equations (4)–(8) were each used, to yield five separate simulations for comparison. The Grashof and Prandtl numbers for each simulation were:

Equation	Grashof number	Prandtl number
4	3.11×10^3	42 100
5	6.79×10^7	285
6	6.79×10^7	285
7	3.80×10^4	12 000
8	3.80×10^8	120.

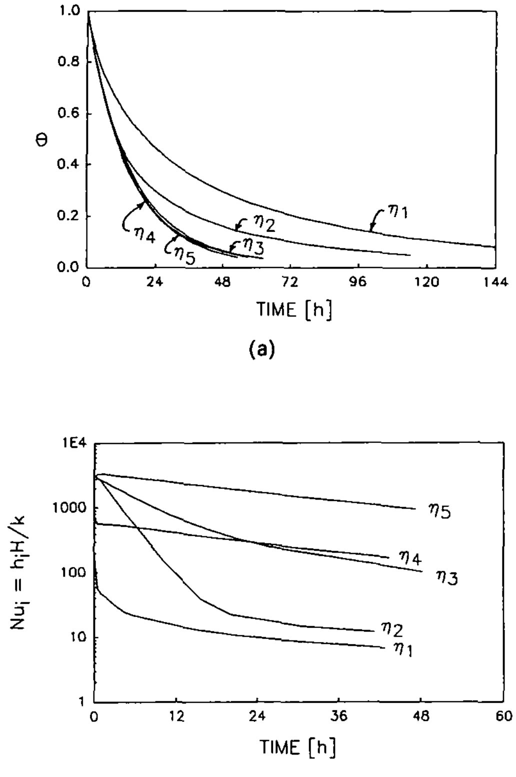

FIG. 7. The effect of the apparent viscosity on cooling: (a) the mean tank temperature vs time; and (b) the internal sidewall Nusselt number versus time.

The mean tank temperature behaviour over time for these simulations is shown in Fig. 7(a). Initially, all the simulations appear to cool at the same rate. The simulation utilizing equation (4) is the first to slow down in the rate of heat loss, since it starts with a relatively high apparent viscosity which then increases as it cools. The simulation using equation (5) is now clearly distinguishable, and it is the next to exhibit a slowdown in the rate of heat loss compared to the others. This equation describes a fluid whose viscosity is initially low (10 mPa s) but increases with a temperature decrease at the greatest rate studied here.

The three remaining cooling profiles are very similar. It is evident that the gentle increase in viscosity with cooling that is characterized by equation (6) has little effect on the overall rate of heat loss. As well, comparing the results of equation (7) with those of equation (8), it seems that a two order of magnitude increase in a constant viscosity does not have an appreciable effect on the cooling rate. This suggests that for these cases, the limiting factor in the rate of heat loss is not the convection in the tank, which is affected by the change in viscosity.

The behaviour of the sidewall internal Nusselt number over the time is shown in Fig. 7(b). This Nusselt number yields a measure of the rate of heat transfer at the interior of the sidewall. The transient nature of the flow is evident from this figure. The simulations utilizing a constant viscosity relationship (equations (7) and (8), corresponding to η_4 and η_5, respectively) show only a gentle decrease in the Nusselt number over time with a relatively constant slope. The rate of heat transfer at the sidewall interior decreases in these two cases solely because the driving force for convection decreases as the tank cools. The Nusselt number for the simulation using equation (8) is larger than that of equation (7) since the lower viscosity permits a more vigorous flow.

In contrast to the two constant viscosity cases, the simulations utilizing a temperature-dependent viscosity relationship exhibit a more complex decay in the Nusselt number over time. The decay can be attributed to both the decrease in the driving force for convection as the tank cools and the concomitant increase in fluid viscosity with cooling. The simulation utilizing equation (4), which has the high initial viscosity as well as being temperature-dependent, shows the lowest sidewall Nusselt number. The apparent viscosity relationship given by equation (5) is the most strongly temperature-dependent, though the initial viscosity is relatively low. The pronounced decrease in the Nusselt number over time for this simulation reflects the inhibiting effect that the varying viscosity has on the flow and thus the rate of heat loss at the sidewall. A similar effect is noted with the simulation using equation (6), though less marked, reflecting the weaker temperature-dependence in the viscosity relationship.

A comparison of the convective flow patterns in the tank for each simulation shows that the patterns remain qualitatively the same, each displaying a clockwise cell driven by the sidewall heat loss and a smaller counterclockwise cell in the top centreline region. However, the fluid viscosity relationship does have

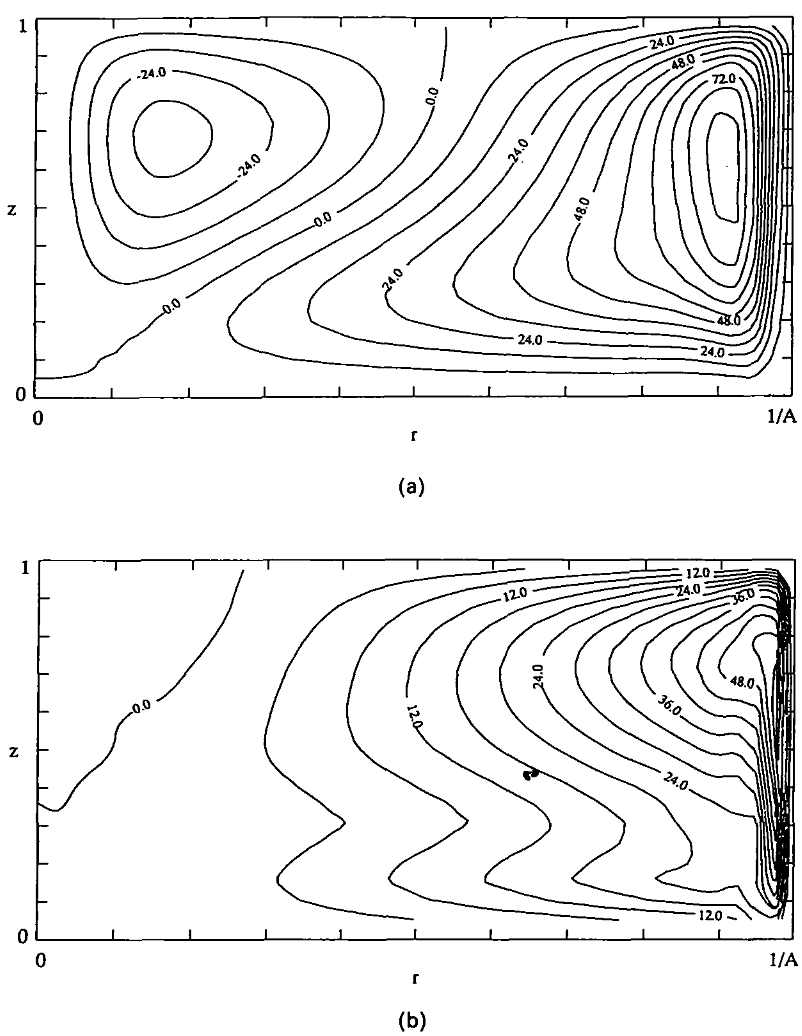

FIG. 8. A comparison of streamlines after 30 min for a simulation using: (a) equation (4), where contours are $\psi \times 10^5$; and (b) equation (8), where contours are $\psi \times 10^4$.

some effect on the velocities and their temporal behaviour.

Figures 8 shows streamlines after 30 min for the simulations using equations (4) and (8), respectively, the two extremes in viscosity relationships studied here. A comparison between figures of the location of the vortex of the clockwise cell near the wall shows one effect of the viscosity. In Fig. 8(a), which shows the simulation where the initial viscosity is relatively high, this vortex is located farther from the wall than with the lower viscosity case depicted in Fig. 8(b). Since this vortex locates the point where flow directions reverse, it is evident that one effect of decreasing the apparent viscosity is to make the wall boundary-layer thinner. This is expected from a vertical-plate analogy.

The conspicuous differences in the gradients in the streamlines near the wall indicates differences in velocities between simulations. The maximum vertical velocity downward at the wall ranges from 1 mm s^{-1} for the simulation corresponding to equation (4), to greater than 6 mm s^{-1} for equation (8), with the ordering consistent with the conclusion that higher viscosities result in lower velocities.

The shapes of isotherms for each simulation were found to be qualitatively similar, as one would expect from the similarity of the flow patterns. In each case a relatively steep temperature gradient exists at the sidewall, a stable temperature gradient is found along the bottom and an unstable gradient is noted near the top surface. The variable viscosity results in a steeper temperature gradient near the sidewall, indicating a thinner thermal boundary layer along with the previously mentioned thinner momentum boundary layer. In general, overall temperature gradients inside the tank were found to be smaller in magnitude for the lower viscosity cases due to more effective mixing attributable to the enhanced flow.

In summary, the effect of the fluid viscosity on the simulation results appears to depend upon the magnitude of the viscosity differences. An increase in the viscosity of two orders of magnitude results in somewhat lower velocities but essentially the same overall rate of cooling.

The implementation of a temperature-dependent apparent viscosity in the natural convection simulator can have significant effects on the results. If the change in the viscosity with temperature is considerable, the fluid flow inside the tank is inhibited and as a consequence the rate of heat loss from the tank decreases from the stirred-tank rate towards the conduction rate. This lower rate of heat loss is not predicted with the constant viscosity relationship, so that choosing an intermediate temperature (film temperature) at which to evaluate the viscosity will inevitably lead to a poor estimation of the rate of cooling for a fluid whose viscosity changes significantly with temperature.

CONCLUSIONS

In this work, a numerical simulator has been developed which predicts cooling rates and flow patterns for the unsteady natural convection of a warm crude oil in a cylindrical storage tank located in a cold environment. The simulator allows for an arbitrary continuous viscosity–temperature relationship to be used to account for increases in viscosity associated with cooling.

It appears that a fivefold increase in the magnitude of the wall heat transfer coefficient has some influence on the rate of cooling of the tank contents but has little effect on the flow structure. However, from the mean tank temperature plots it is evident that over a long period of time even this effect is diminished. The tank contents cool to the ambient temperature asymptotically, and the effect of the wall heat transfer coefficient on the rate of heat loss is most pronounced in the early stages of cooling.

A numerical simulation has been performed of the natural convection of a crude oil initially at 20°C contained in a cylindrical tank in an environment at −30°C. The effect of the tank aspect ratio was found to be that the 'taller' tanks cooled more quickly than the 'short' tanks, as was expected since the rate of heat loss at the sidewall was larger than that at the top and bottom. For the aspect ratio of two, only a single convection cell developed in the radial plane, as compared with two cells for the aspect ratios of one-quarter, one-half and one.

The effect of the apparent viscosity of the fluid was examined using five different viscosity–temperature relationships. Decreasing the magnitude of the apparent viscosity resulted in an increase in the magnitudes of the convection velocities. For the case of constant viscosity, an increase in the viscosity of two orders of magnitude did not significantly alter the rate of heat loss, suggesting that effective mixing occurred in both cases. However, the rate of heat loss is significantly affected when the viscosity is temperature dependent, provided that the change in viscosity with temperature is dramatic.

Acknowledgements—The authors gratefully acknowledge the support of the Natural Sciences and Engineering Research Council in this work, through the Operating, Strategic and Scholarship programs. In addition, the authors express gratitude to Panarctic Oils Ltd. for the supply of Benthorn crude oil and for advice with regard to a typical field storage scenario.

REFERENCES

1. M. A. Cotter and M. E. Charles, Transient cooling of petroleum by natural convection in cylindrical storage tanks—I. Development and testing of a numerical simulator, *Int. J. Heat Mass Transfer* **36**, 2165–2174 (1993).
2. M. A. Cotter, Transient natural convection in petroleum storage tanks, Ph.D. Thesis, University of Toronto, Toronto (1991).